

# Assessment and Correlation of Seasonal Changes in Subsurface Resistivity over a Region along Zaria, Northwestern Nigeria

Bamidele S.Y.<sup>1\*</sup>, Usman A.<sup>2</sup>, Momoh K.O.<sup>3</sup>, Lawan A.M.<sup>4</sup>

<sup>1,3</sup>Department of Physics Ahmadu Bello University Zaria, Nigeria

<sup>2</sup>Department of Physics Kebbi State University of Science and Technology Aliero

<sup>4</sup>Department of Geology, Skyline University Kano, Nigeria

DOI: [10.36348/sjet.2022.v07i01.005](https://doi.org/10.36348/sjet.2022.v07i01.005)

| Received: 10.12.2021 | Accepted: 23.01.2022 | Published: 30.01.2022

\*Corresponding author: Bamidele S.Y

Department of Physics Ahmadu Bello University Zaria, Nigeria

## Abstract

Vertical electrical sounding was conducted using Schlumberger array at Ahmadu Bello University site II with the aim to determine seasonal changes in subsurface resistivity. A maximum current electrode spacing of 200 m was used for this survey and measurements were taken twice a month for one year. The acquired data was processed using IPI2win software and subsequently used to determine geoelectric sections. Five geoelectric layers were obtained from the interpretations. The first two geoelectric sections form the overburden with thicknesses ranging from 0 – 11 m and resistivity ranging from 122 to 200  $\Omega\text{m}$ . The third and the fourth geoelectric layers were interpreted as the weathered basement with thicknesses ranging from 11 – 24 m and resistivity ranging from 178 to 363  $\Omega\text{m}$  while the last layer was interpreted as the fresh basement with resistivity ranging from 422 to 1574  $\Omega\text{m}$ . Comparing the depth of interpretation of data in both seasons, the wet season data shows more depth probing which is fairly stable; this could be because the earth subsurface was more saturated and hence more conductive. The dry season data interpretation shows more stability compared to that of the wet data depth interpretation. A strong correlation was obtained from the statistical analysis between depth interpretations of the dry and wet season. A linear regression equation was obtained as  $y = 1.0684x - 0.2188$  and about 99.97% dependence which show that we can use the wet season depth information to determine that of dry. The wet season is more appropriate for more depth probing with the exception of searching for water table since it rises up during the wet season and that may not be the true water table, while the dry season is appropriate for stability in data acquisition when required in a survey.

**Keywords:** Resistivity; Subsurface; Geophysical Survey; Geoelectric section; Schlumberger configuration.

**Copyright © 2022 The Author(s):** This is an open-access article distributed under the terms of the Creative Commons Attribution 4.0 International License (CC BY-NC 4.0) which permits unrestricted use, distribution, and reproduction in any medium for non-commercial use provided the original author and source are credited.

## 1.1 INTRODUCTION

There have been arguments between researchers with respect to the best season to acquire resistivity data for the purpose of spatial studies. This survey has bridge the gap about the argument, by determining the best season to acquire resistivity data for spatial studies. Electrical imaging surveys are now widely used to map areas with complex subsurface geology.

The many applications include groundwater exploration, mineral exploration, environmental and engineering studies (Griffiths and Baker, 1993).

Electrical resistivity which is an artificial source geophysical method, involves investigation of variations of electrical resistivity, by causing an

electrical current to flow through the subsurface of the earth using wires (electrodes) connected to the ground. Most rock-forming minerals are very poor conductors, and ground currents are therefore carried mainly by ions in the pore waters. Pure water is ionized to only a very small extent and the electrical conductivity of pore waters depends on the presence of dissolved salts, mainly sodium chloride. Clay minerals are ionically active and clays conduct well if even slightly moist (Milson, 2003). The subsurface water table is the upper boundary of saturated subsurface water or aquifer zone, whereby the pressure in this boundary equals that of the atmosphere (He *et al.*, 2002). The fluctuation in water table depths is related to the weather climate condition. In the dry periods with low precipitation, water table depths were low but become higher in the wet seasons. According to Haridjaja and Herudjito (1979),

precipitation falls from the air in solid or liquid form such as rain, snow, ice, mist or vapour to the earth surface (He *et al.*, 2002). Water table dynamics is determined by the balance of recharge and discharge of water. The main sources of water recharge are precipitation and soil water ground flow, whereas the main sources of water discharge are evapotranspiration and drainage. Water table changes are very responsive to recharge (mainly precipitation) and discharge (mainly evapotranspiration).

Electrical resistivity method has been successfully used by researchers in identifying and delineating different geoelectric layers and detecting isolated bodies of anomalous resistivity. A principal advantage of the electrical resistivity method is that quantitative modeling is possible using either computer software or published master curves. The resulting models can provide accurate estimates of depths, thicknesses, and electrical resistivity of subsurface layers (Ojo *et al.*, 2014). (Abdus SALAM *et al.*, 2015),

conducted a survey of measuring soil resistivity and ground resistivity for dry and wet soil at Gadong 66kV substation of Brunei Muara district, he concluded that the values of observed resistance and the calculated resistance using Cymgrd simulation software matched closely considering the wet soil while the calculated dry soil resistivity value was found to be higher than the observed value because of high resistance encountered.

### 1.2 Location of the Study area

The study area is located at Ahmadu Bello University Zaria, Samaru site II, main campus, Kaduna state, Nigeria. It lies between Longitudes  $07^{\circ} 38' 25.66''\text{E}$  to  $07^{\circ} 38' 31.11''\text{E}$ , and Latitudes  $11^{\circ} 08' 13.14''\text{N}$  to  $11^{\circ} 08' 19.71''\text{N}$ . And the coordinate of the point where measurement was carried out is  $11^{\circ} 08' 14.6''\text{N}$  and  $07^{\circ} 38' 29.02''\text{E}$ . Figure 1.1 shows google earth map of the site in the study area. Peg 1, 2, 3, 4 represent the coordinates stated above while the red peg represents the sounding or VES point.

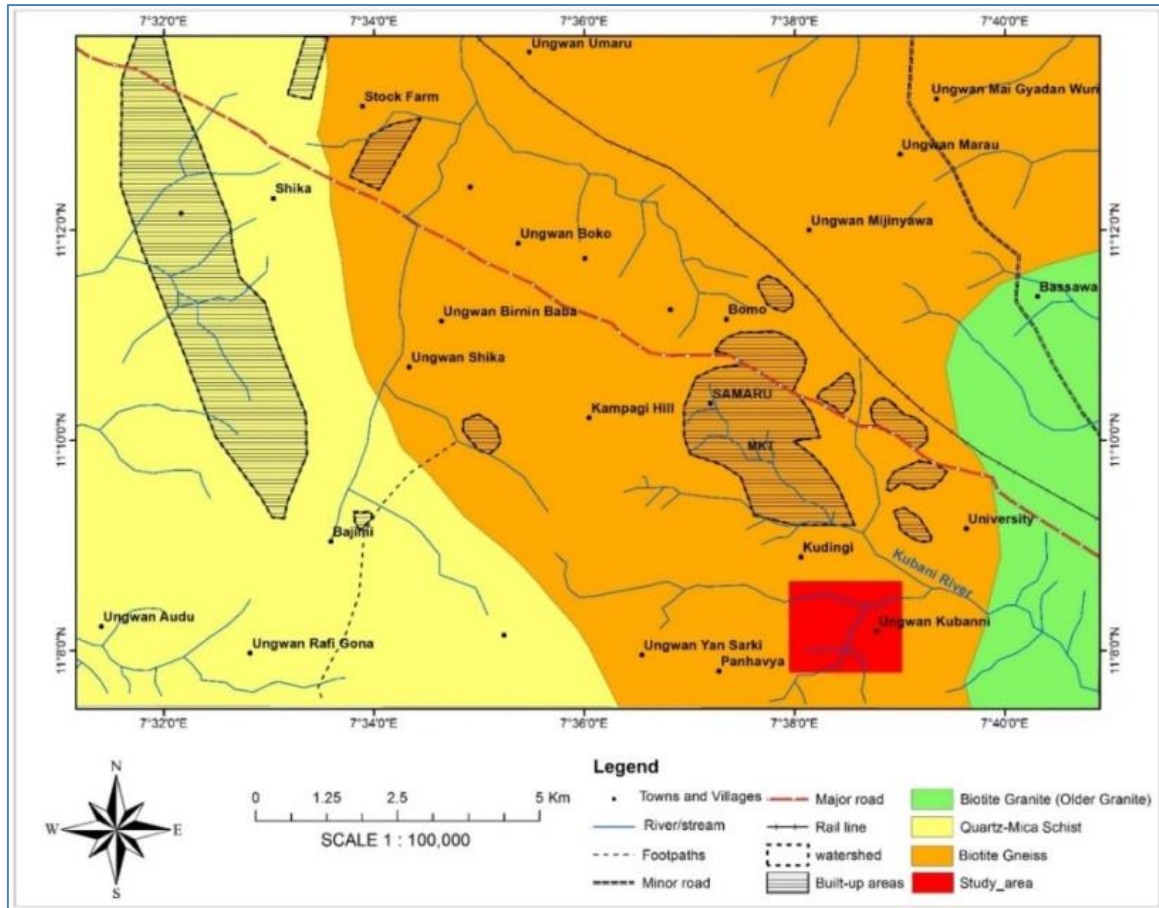


Fig-1.1: Google Earth Map showing the location of the study area. (Courtesy Google Earth).

### 1.3 Geology of the Study area

The geology of the study area can be shown in figure 1.2. The site is situated in Ahmadu Bello University main campus, Samaru, (Zaria, Kaduna State of Nigeria) which occupies 9% area of Kubanni River Basin and positioned on the North-Western part of the basin (figure 1.2). The study area is part of the NW basement terrain underlain by basement rocks of Precambrian age. They are mainly granites, gneisses, and schists. Oyawoye (1964) showed that there is a structural relationship between this Basement Complex and the rest of the West African basement. This is partly due to the fact that the whole region was involved in a single set of the orogenic episode, the Pan African orogeny, which left an imprint of structural similarity upon the rock units. The gneisses are found as small belts within the granite intrusions and are also found

east and west of the batholiths (McCurry, 1970). The biotite gneiss extends westwards to form a gradational boundary with the schist belt. The gneiss continues eastwards to some extent and is occasionally broken up by the Older Granite (Wright and McCurry, 1970). The basin is underlain by rocks of the Precambrian age. Biotitic gneiss predominates in the area and outcrops, mainly in the stream valley where they are deeply weathered (Wright, 1970). The biotitic gneiss complex consists of medium to coarse grains and moderates of weakly foliated rocks which constitute about 30-40% of the basement complex exposed in the basin (Wright and McCurry, 1970). Eigbejo (1978) stated that two phases of deformation took place in the basin: one along the E-W axis while the second was roughly along the N-W axis. The later was so strong that it obliterated evidence of the former and left a dominant N-W structure trend.



**Fig-1.2: Geological map of the Kubanni Basin (Modified from McCurry, 1973 and Eiggbefo, 1978)**

**2.0 Basic Theory**

In an electrical resistivity survey, an electric current is introduced to the ground by means of two current electrodes. The current set up a stationary current field, and because of the ohmic potential drop, an electrical potential field is also created and this field gets distorted in the neighborhood of a subsurface zone of anomalous conductivity. The aim of the electrical

resistivity survey is to search for such anomalous zones in the electrical field with a pair of potential electrodes. The basic assumption is that current flow in the potential measuring circuit is negligible compared with the current flow in the ground so that the potential electrodes themselves will have no disturbing effect upon the electrical field (Grant and West, 1965).

For two-point current electrodes on the earth’s surface, the potential difference  $\Delta U$ , between potential electrodes

$$\Delta U = \frac{I\rho}{2\pi} \left[ \frac{1}{r_1} - \frac{1}{r_2} - \frac{1}{r_3} + \frac{1}{r_4} \right] \tag{1}$$

Such an arrangement corresponds to the four electrodes spread normally used in resistivity fieldwork, where  $\rho$  is the resistivity,  $I$  is the current and  $r_1, r_2, r_3,$

and  $r_4,$  are the inter-electrode distances as can be seen in figure 3.

From equation (1), the apparent resistivity can be represented as;

$$\rho_a = \frac{\Delta U}{I} \frac{2\pi}{\left[ \frac{1}{r_1} - \frac{1}{r_2} - \frac{1}{r_3} + \frac{1}{r_4} \right]} \tag{2}$$

Where 
$$K = \frac{2\pi}{\left[ \frac{1}{r_1} - \frac{1}{r_2} - \frac{1}{r_3} + \frac{1}{r_4} \right]} \tag{3}$$

$$\rho_a = K \frac{\Delta U}{I} \tag{4}$$

The result is independent of the position of the electrodes and is not affected when the current and the potential electrodes are interchanged.

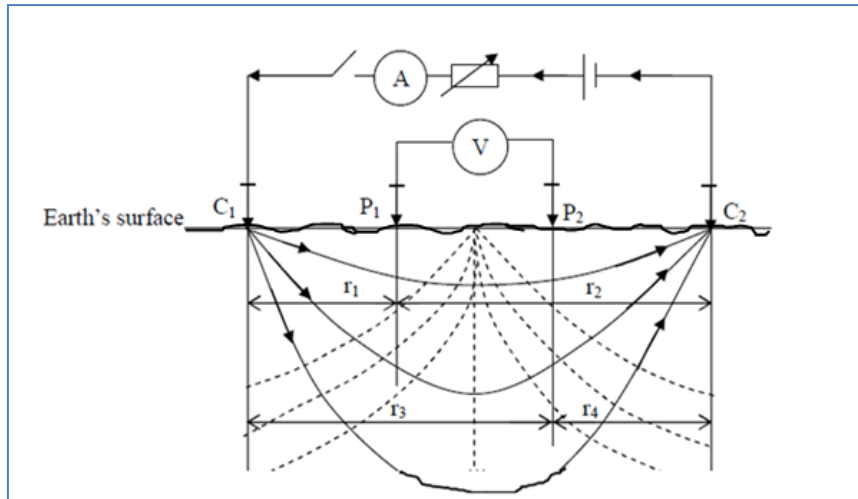


**Fig-3: General four-electrode configuration. (Telford *et al.*, 1990)**

### 3.0 MATERIALS AND METHOD

#### 3.1 Materials

The Petrozenith Terrameter (PZ-03) (Plate 1) is a one dimensional (1D) Resistivity (VES) and or Spontaneous Potential (SP) measuring instrument. It has four electrode channels, reset button, a selection key, a plug switch for A.C charging, menu button, ON and OFF switch button and a power connector input for D.C charging. The four-electrode channel; two current electrodes (red channels) and two potential electrodes (black channels). The selection button is used to select

either Resistivity or SP measurement, the number of cycle of measurement, current, sleep mode timing to save battery if not in use. The Terrameter is also accompanied by four reels of cable for electric contact between the Terrameter and the ground through the metal electrodes. The electrode switching is manual unlike the Terrameter SAS 4000 that uses automatic electrode selector to switch from one electrode to another.



**Plate-1: Picture showing the Petrozenith Terrameter and some other instrument that was used for the survey**

#### 3.2 METHODOLOGY

Petrozenith Terrameter was used to acquire Electrical Resistivity Data. The Schlumberger array was used for the survey. This array was adopted because it has an advantage over the Werner array in that the problem of dragging the electrodes and the instrument along a large surface area will be eliminated. The survey was carried out using a 1D resistivity method

with a single spread. The measurement was taken twice each month with the spread along East to West direction of the study area, maintaining a fixed center (the red peg in figure. 4) throughout the data collection in the dry and wet season. Figure 4 shows details about the site such as the location of the borehole, the profile trend which has a length of 200 m (line A to B) i.e. a probing of about 100 m downwards.

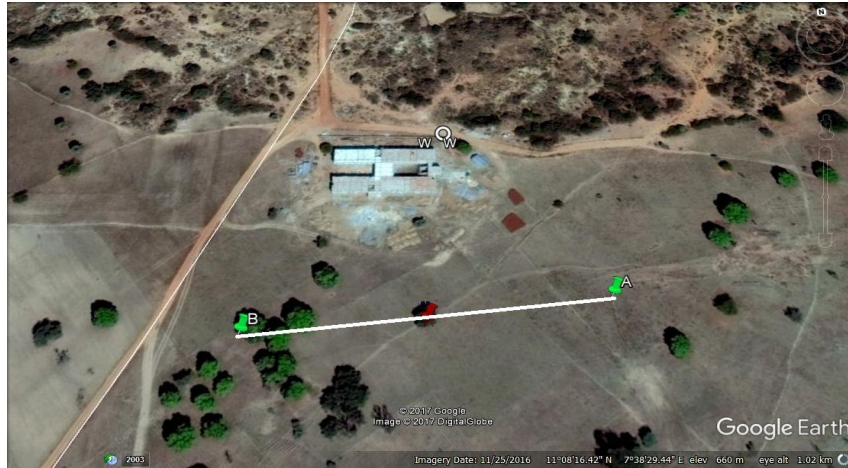


**Fig-4: Google Earth Map showing the spread direction that was used and the position of the borehole (WW) dug at the site. (Courtesy Google Earth).**

The peg A and B figure 4, represent the extent (length) of the spread while the red peg was the sounding point or VES point. Data was carried out at these same points throughout the survey for 12 months, twice in a month. The profile was mapped out using a compass and a tap-rule in order to achieve a straight line and exact length of about 200 m for the profile. The Petrozennith terrameter was then placed at the sounding point and then two metal electrodes were driven into the ground (about 1/3 of it) and were labeled the potential electrode with equal distance away from the sounding point. Afterward, another two metal electrodes were driven into the ground (about 1/3 of it) farther away from the potential electrodes with equal distance apart

and were labeled the current electrodes. The Terrameter was then connected to these electrodes using respective connection wires, i.e. potential wires connected to potential electrodes while the current wires were connected to the current electrodes too. The Terrameter is then turned ON and set to resistivity measurement. The 'GO' button was pressed to start taking readings and the values were recorded. These were repeated for sets of inter-electrode spacing throughout the profile. This methodology was adopted for all data taking on the site for both dry and wet seasons.

#### 4.0 RESULTS

**Table-1: The depth interpretation of each layer from the geoelectric sections**

DATA SET NUMBER	Depth for Layer 1 (m)	Depth for Layer 2 (m)	Depth for Layer 3 (m)	Depth for Layer 4 (m)
1	2.48	7.5	17.6	55
2	2.45	7.5	17.6	55
3	2.51	7.6	17.8	55
4	2.51	7.6	17.9	55.6
5	2.51	7.6	17.8	55.6
6	2.51	7.6	17.8	55.6
7	2.51	7.6	17.8	55.6
8	1.51	6.5	16.6	54.3
9	1.52	6.58	17.5	55.3
10	2.51	7.59	32.7	83.2
11	2.51	7.59	22.6	73.3
12	1.51	6.61	21.9	72.4
13	2.51	10.1	35.1	85.1
14	2.51	10.1	20.2	70.8
15	5.01	15.1	40.3	91.2
16	2.51	7.6	32.7	83.2
17	2.51	7.6	32.7	83.2
18	2.51	7.6	32.7	83.2
19	2.51	7.6	32.7	83.2
20	2.51	12.6	38	89.1
21	2.51	10.1	35.1	85.1
22	2.51	10	35.1	86
23	2.51	10	35.4	86
24	2.5	10	35.4	86

A total of 24 resistivity data set was collected within the two seasons (wet and dry season) at one sounding point. The interpretation of the data that was processed using IPI2win as shown in figure 5, 6 and 7.

However, only the curves of data sets 1, 9, 22 from table 1 are represented, depicting periods of the year; before rainfall (1), during rainfall (9) and after rainfall (22).

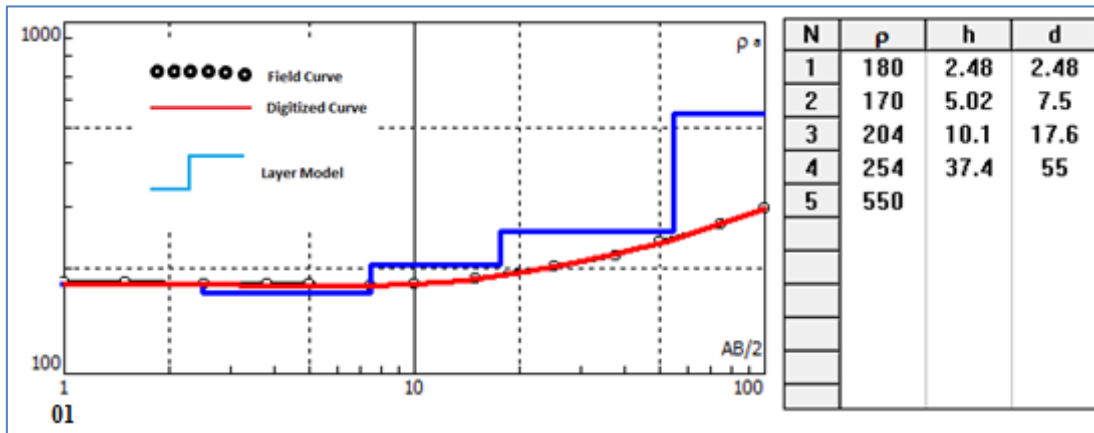


Fig-5: Resistivity interpretation for data set 1 (5<sup>th</sup> January, 2018)

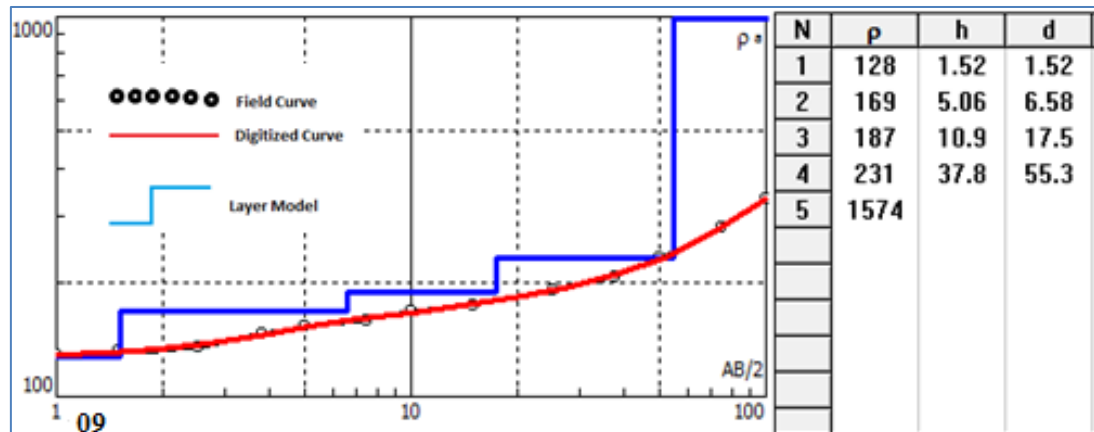


Fig-6: Resistivity interpretation for data set 9 (5<sup>th</sup> May, 2017)

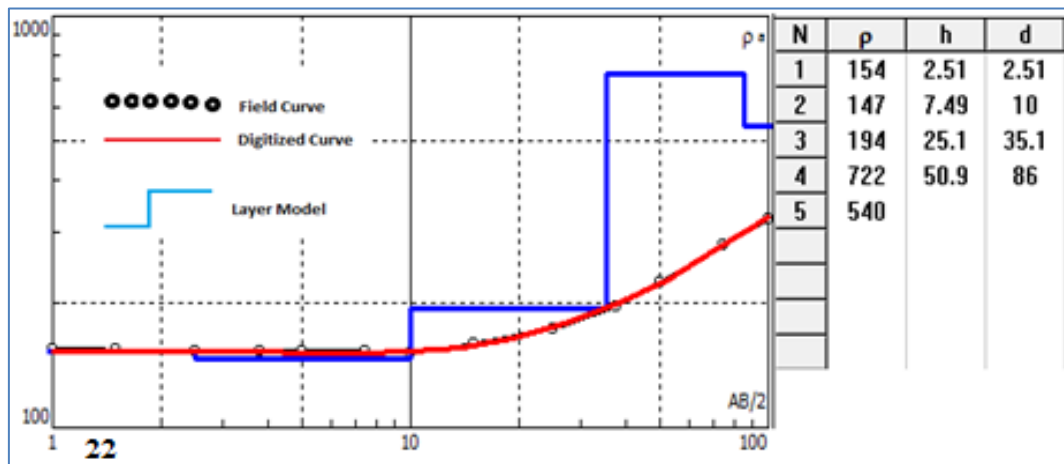


Fig-7: Resistivity interpretation for data set 22 (22<sup>nd</sup> November, 2017)

The depth and resistivity results acquired from the data sets interpretations are plotted below in figure 8 and 9.

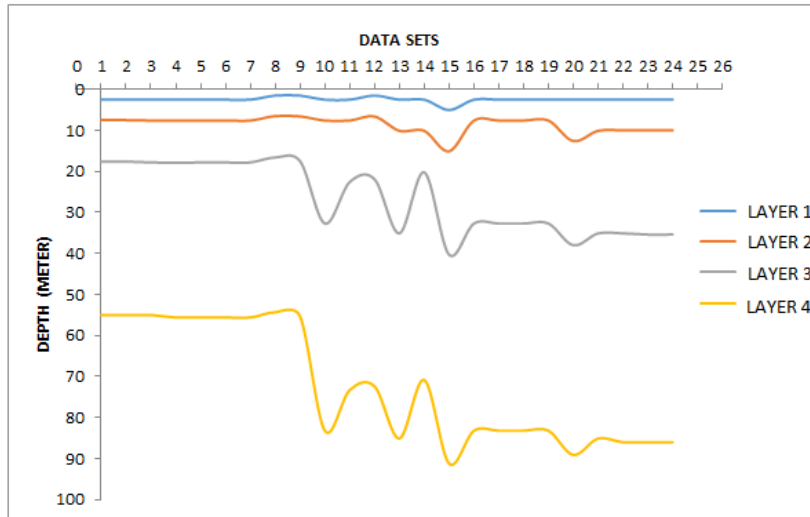


Fig-8: A plot of data set showing depth to layer variation from dry season to wet season for data collected at the site.

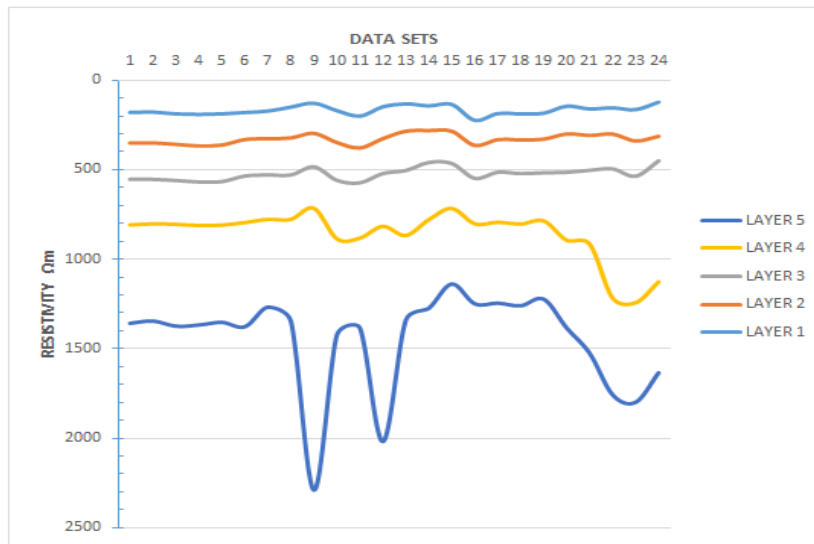


Fig-9: Layer resistivity distribution

The interpreted data (geoelectrical sections) shows five (5) number of layers ‘n’, with the resistivities as: layer 1 resistivity ( $\rho_1$ ) ranges from 122 to 224  $\Omega m$ , layer 2 resistivity ( $\rho_2$ ) ranges from 140 to 191  $\Omega m$ , layer 3 resistivity ( $\rho_3$ ) ranges from 137 to 211

$\Omega m$ , layer 4 resistivity ( $\rho_4$ ) ranges from 231 to 722  $\Omega m$  and lastly layer 5 resistivity ( $\rho_5$ ) ranges from 422 to 1574  $\Omega m$ . The layer thickness ‘h’ ranges as;  $h_1 = 0$  to 2.5 m,  $h_2 = 2.5$  to 15.1 m,  $h_3 = 15.1$  to 40.3 m and  $h_4$  begins from 40.3 m downwards.

Table-2: Lithology of the site as inferred from the interpretation of the 24 data sets using the borehole data as a guide.

Depth (m) From	To (m)	Thickness (m)	Interpreted Lithology	Hydrological Characteristics
Overburden 0 – 11m				
0	5	5	Sandy Topsoils	
5	11	6	Brownish red Sandy Clay	
Weathered Basement 11 - 24m				
11	24	13	Grayish brown, Sandy soil, Mottled clay, Coarse to medium-grained sand	Aquifer
Fresh Basement 24 – 31m				
24	31	7	Fractured Basement	Aquifer

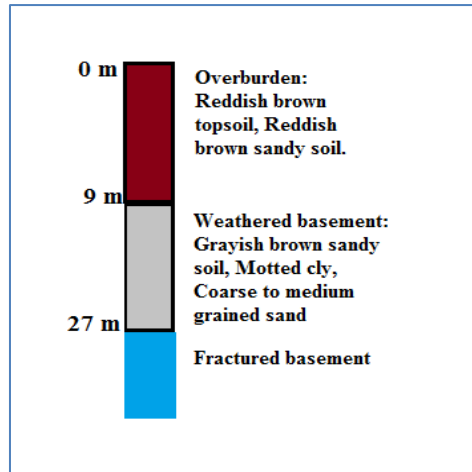


Fig-10: Borehole log of Akenzua Hostel (modified from momoh *et al.*, 2019).

Statistical analysis was done on the acquired information of geoelectric sections of table 1. Correlation and regression analysis were taken into consideration. The resistivity information was considered first to see how much it varies from dry season to wet season. This was done by adding up the

resistivities for each layer and take the average for the dry season and then the wet season. A table that shows the information plotted can be seen in table 3. The results were then plotted against each other. Figure 11, shows the plot of these values from different seasons.

Table-3: Shows averaged resistivity for both seasons.

	AVERAGE RESISTIVITY FOR DRY SEASON ( $\Omega m$ )	AVERAGE RESISTIVITY FOR WET SEASON ( $\Omega m$ )
LAYER 1	173.7647	150.8571
LAYER 2	160.7059	163.4286
LAYER 3	194.5294	195
LAYER 4	351.1765	299.4286
LAYER 5	523.4706	743.4286

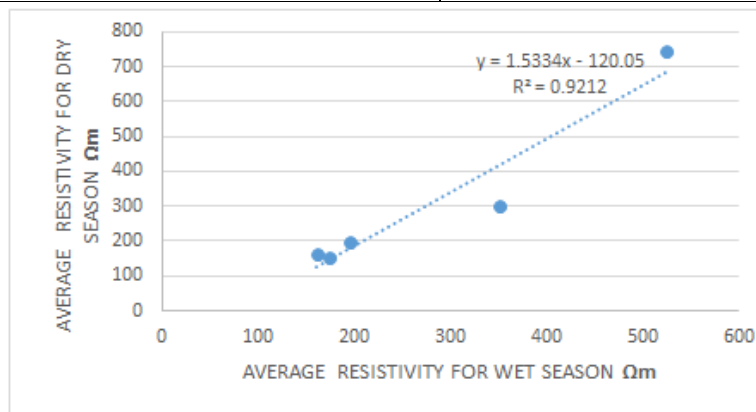


Fig-11: A plot of average resistivities of the dry season against wet

The depth interpretation obtained from geoelectrical section was also summed up and average for each layer in the dry season and then in the wet

season. This result can be seen in table 4. The result was plotted against each other to observe their correlations as seen in figure 12.

Table-4: Shows the averaged depth information for both seasons.

	AVERAGE DEPTH FOR DRY SEASON (m)	AVERAGE DEPTH FOR WET SEASON (m)
LAYER 1	2.45	2.58
LAYER 2	8.3	9.1
LAYER 3	26.51	27.19
LAYER 4	70.98	75.9

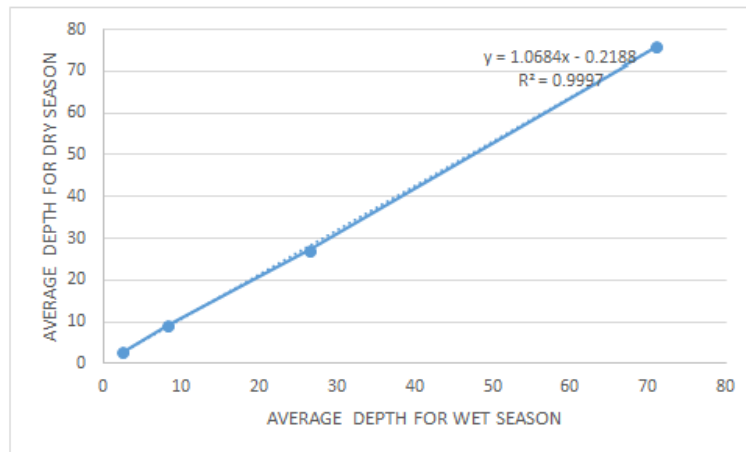


**Fig-12: A plot of average depth information of dry and wet season**

Figure 12. shows a plot of average depth information gotten from the geoelectrical sections of both dry and wet season. It can be seen that their depth information correlates well since all the points lie on a straight line. A linear equation was also generated as;  $y = 1.0684x - 0.2188$  and a square of residue as 0.9997.

#### 4.1 DISCUSSION

The first and second layer of geoelectric sections correlates with the overburden layer of geological section obtained from the borehole data of thickness 0 – 11 m with resistivity range of 122 to 200  $\Omega\text{m}$ , while the third and fourth layer correlates with the weathered basement of borehole data of thickness from 11 – 24 m with resistivity range of 178 to 363  $\Omega\text{m}$  and lastly the fifth layer was characterized as the fresh basement. The wet season data fit well with the borehole log of Akenzua Hostel than the dry season data which is in line with the conclusion of Abdus SALAM *et al.* (2015). Also, the wet season has more depth probing when compared to the data collected during the dry season. Also the weathered and the overburden layer contains some clay material which reduces porosity, this means reduced permeability and thus increased resistivity. This accounted for more probing depth in the wet season VES data interpretation. The average resistivity of the dry season fairly correlates with that of the wet season. The average depth interpretation plot of the dry and wet season correlates very well which means an increase in the depth of the dry season results to a change in the wet season. The square of residue when multiplied by 100 gives the percentage of dependency on the model acquired from the correlation of depths. About 99.97% dependence was recorded which in turn means we can actually use depth data acquired during the wet season to determine that of dry season depth of a particular place.

#### 4.2 CONCLUSION

The resistivity of layers from both seasons agrees with the resistivity of materials and or rock

found in the geologic borehole logs of Akenzua Hostel of Ahmadu Bello University used for correlation. The depth analyses, collected from the interpretation of the data from wet season fits perfectly with the depth analysis of the borehole log in that the depth ranges for the overburden, weathered basement and fractured basement are equal. With these few reasons, it can be suggested that the wet season is best appropriate for collecting resistivity data that deals with deeper depth probing with the exception of searching for water table because during the raining season, the water table rises up and gives false water table which may dry up during the dry season. While the dry season is best suited for stability in the data acquisition. The weathered basement which has a thickness of about 11.0 to 24.0 m can be related to the work of Osumeje (2008) which says that the weathered basement thickness is within the range of 9.0 to 30 m.

#### REFERENCE

- Salam, M. A., Rahman, Q. M., Ang, S. P., & Fushuan, W. E. N. (2017). Soil resistivity and ground resistance for dry and wet soil. *Journal of Modern Power Systems and Clean Energy*, 5(2), 290-297.
- Eigbejo, C. (1978). Hydrogeology of the Kubanni Drainage Basin, Zaria. *Unpublished M. Sc. Thesis, Department of Geology, Ahmadu Bello University, Zaria. Geology and Metallurgy, 1, 87-102.*
- Grant, F.S. and West, G.E. (1965) Interpretation Theory in Applied Geophysics. *McGraw-Hill, New York.*
- Griffiths, D.H., & Barker, R.D. (1993). Two Dimensional Resistivity Imaging and Modeling in Areas of Complex Geology. *Journal of Applied Geophysics, 29, 211-226.*
- Haridjaja, O., & D. Herudjito. (1979). Physical Maturity and Level of Mineral Decomposition of Peat Soil in Relation to Some Physical Properties of Soil Intertidal Reef Court, South Sumatra. *Proceedings of Symposium Nasional III, Tidal Regional Development, Book II, (TRD'79), Indonesia, 428-437.*

- 
- He, X., M.J. Vepraskas, R.W. Skaggs and D.L. Lindbo, 2002. Adapting a Drainage Model to Simulate Water Table levels in Coastal Plain Soils. *Soil Sci. Am. J.*, 66: 1722-1731.
  - McCurry, P. 1970. "The Geology of Zaria Sheet 21". *unpublished M.Sc. Thesis, Department of Geology, Ahmadu Bello University, Zaria.* 26
  - McCurry, P. 1973. "The Geology of Zaria Sheet 21". *H.M stationery Office, ISBN 0118806130, 9780118806138.*
  - Milsom, J. (2003) "Applied Geophysics," 3rd edition, John Wiley & Sons Ltd., pp83-126 Mining, Retrieved from <http://creativecommons.org/licenses/by/4.0/>
  - Momoh, K.O., Raimi, J., Lawal, K.M (2019). Seismic refraction survey for foundation investigation at Ahmadu Bello University Zaria Phase II, Kaduna State, Nigeria. *FUDA Journal of Science*, 3(3), 161 – 167.
  - Offodile, M.E. (1992). An Approach to Groundwater Study and Development in Nigeria. *Mecon Eng. Services Ltd. Jos, Nigeria 1st edition, pp144-155.*
  - Ojo O, Toyin, O., & Olorunyomi. J. (2014). Determination of Location and Depth of Mineral Rock at Olode Village in Ibadan, Oyo State, Nigeria, Using Geophysical methods.
  - Osumeje. (2008). Correlation of Seismic Section with Geologic Borehole Logs in Some Student Hostels at Ahmadu Bello University (main campus), Zaria, Kaduna State. *Unpublished thesis M.Sc. thesis, Department of Physics, Ahmadu Bello University, Zaria.*
  - Oyawoye, P. O. (1964). "Geology of Nigerian Basement Complex". *Journal of Mining and Geology, 1, 110-121.*
  - Telford, W.M., Geldart, L.P., Sheriff, R.E. (1990). *Applied Geophysics, Cambridge: Cambridge University Press.*
  - Wright, J. B., & McCurry, P. (1970). "The Geology of Nigeria Sheet 102 SW, Zaria and its Regions. Edited by M. J. Mortimore. Department of Geography, Occasional paper, No.4, Ahmadu Bello University, Zaria.
  - Wright, J. B. (1970). Control of mineralization in the older and younger tin fields of Nigeria. *Economic geology, 65, 945 – 951.*